View metadata, citation and similar papers at core.ac.uk
brought to you by CORE
provided by Loughborough University Institutional Repository

Presented at the Photovoltaic Science, Applications and Technology (PVSAT-12) conference
6-8 April 2016, University of Liverpool, Liverpool, UK

Development of a Solar Cell Spectral Response Mapping System using Multi-LBIC Excitation

M. Bliss*, G. Koutsourakis, T.R. Betts, R. Gottschalg

Centre for Renewable Energy Systems Technology (CREST), Wolfson School Mechanical, Electronic and Manufacturing Engineering, Loughborough University, Loughborough, Leicestershire, LE11 3TU, UK
*Corresponding Author M.Bliss@lboro.ac.uk

Abstract

This work presents a new multi-laser LBIC measurement system that is currently under development at CREST. The final set-up uses 11 lasers, 6 of which are currently operational, to form a spatially resolved spectral response map of the device under test. The design aspects of the measurement system are detailed and first measurements of a crystalline and amorphous silicon solar cell are demonstrated. Measurements show how a crack in a crystalline silicon solar cells affects the local quantum efficiency and the effects of discoloration in amorphous silicon. Thus, highlighting the advantages in multi-wavelength and absorption depth profiling of device performance and defects.

1 Introduction

Laser-Beam Induced Current (LBIC) measurements are a spatially resolved laser scanning technique for current mapping of solar cells [1][2]. This technique is used to investigate performance variations within the active area of a solar cell. Even though LBIC measurements are much more time consuming compared to electroluminescence (EL) imaging, these methods are rather complementary to each other and widely used in photovoltaic R&D.

Mapping the local current of a cell using multiple wavelengths over the full response spectrum of the sample means one can investigate the local spectral response (SR) or external quantum efficiency (EQE) of the device. SR is a significant quality indicator of light absorption characteristics of a solar cell. Optical and electrical losses can be determined, as well as local photon absorption properties of the sample. Diffusion length of minority carriers be investigated as well as local short circuit current density (J_{SC}) [1] and depth profiles of performance and defects. A detailed spatially and spectrally resolved investigation of solar cells thus benefits the R&D process of improving device performance and manufacturing processes. Such performance characterisation can also aid towards understanding the ageing mechanisms of devices which are much needed insights to improve lifetime and reliability of PV.

Some localized SR measurement systems use a monochromator based approach. This method can deliver very high resolution measurements but long measurement times makes them often impractical. More advanced measurement systems use multiple light sources at the same time to measure a SR map in a significantly shorter time frame at the expense of finite SR resolution. Light sources used are either Lasers (up to 6 [1]), LEDs (up to 57 reported in [3]) or, as recently reported, a broadband source with digital micro-mirror device (up to 256 bands, [4]).

This work reports the development of an in-house spatially resolved SR measurement system based on 11 lasers, with wavelengths ranging from violet at 405nm to the near infrared region at 1060nm. A multi laser LBIC system that used 2 laser sources has been built at CREST in the past [2]. As other advanced multi-source systems, frequency modulation is utilized to measure lasers simultaneously, which significantly shortens measurement time [5]. The measurement hardware is embedded into the combined global spectral EL measurement system [6] and thus provides the potential to extend the total characterisation capabilities.

In the following, the Multi-LBIC system is described in detail. The first series of measurements from the almost completed system are demonstrated. The results show the capabilities of the system and highlight the importance of localised SR and EQE measurements in device characterisation. The design remarks are discussed and areas of optimisation and extension are identified.

2 Multi-LBIC local SR system

The final measurement system consists of 11 diode lasers: 405, 535, 635, 690, 780, 808, 850, 904, 980, 995 and 1060nm of which the underlined laser wavelengths are already operational. All sources are irradiance controlled via internal or externally mounted photodiode by in-house build control boards. Those sine-wave modulate the laser intensity using a 12bit, 200kS/s signal generator circuitry at any frequency of up to 500Hz. A different frequency for every wavelength is used to allow for simultaneous measurements.

Every laser is coupled with a single mode fibre, all the fibres bundled together and, coupled into a thicker multimode single core fibre, lead to the measurement head (Figure 1). The head contains a 50-50 beamsplitter. The reflected

ISBN 0 904963 82 9

path is used for laser intensity reference measurements and the transmitted focuses the beam on the sample using a microscope objective lens. The spot size is adjustable down to approximately 50µm with a small wavelength dependence. The reflected and emitted light returning from the sample is again partly reflected by the beamsplitter and directed to a photodiode for direct reflectance measurements.

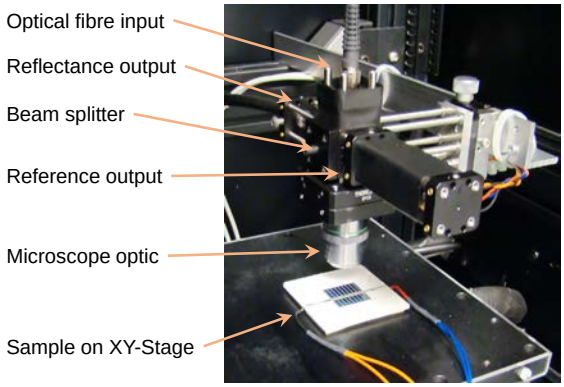

Figure 1: Photograph of the optical measurement head.

The sample under test is 4-wire voltage biased using a source measure unit. The measurement pic-up is realized using an external AC-coupled amplifier for the current measurement of the sample and a trans-impedance amplifier for the reference and reflectance signal diodes. All signals are digitalised using a DAQ card. A simple FFT applied onto the measured signals is used to extract the measurements of every laser at its modulated frequency. At this stage of the development of the system, the SR was preliminarily calibrated using a reference cell with known spectral response.

An XY-stage with temperature controlled sample holder is used to move the sample, while the measurement head is mounted stationary.

3 First Measurements

Initial measurements have been carried out on two samples. A mono-crystalline (c-Si) silicon and an amorphous silicon (a-Si) solar cell. Localised EQE is measured with all 6 lasers operating simultaneously in a frequency range of 220Hz to 320Hz with 20Hz separation. The spot size was adjusted to ~200µm and point data acquisition time was 100ms. Approximately 3.5 points per second are measured at a 200µm resolution (point-point travel distance).

3.1 c-Si solar cell

The mc-Si cell tested is a laminated 20x20mm² device. Measurement resolution is 50µm with a total measurement count of 194k measurements including the border area around the cell. Total measurement time was ~10h. Higher resolution was used for demonstration purposes. A 200µm resolution map would have been finished in ~1h without losing much of the detail.

The main feature apparent from the LBIC maps of the lasers (Figure 2) is the crack formed during the lamination process. This crack is not apparent on measurements below 690nm and is much more pronounced, but also blurred, with increasing wavelengths above 690nm. Since the 405nm violet laser only measures absorption at the surface of the cell, the crack is almost invisible. The deeper the penetration and absorption of light the more pronounced the crack becomes. At 1060nm the crack is very blurry, which is not due to defocussing of the laser but rather due to the longer path of the light before it is absorbed combined with scattering at the surfaces. At long wavelengths one can clearly see the back contact on the back surface field, which is an area with low reflection and thus light is not efficiently absorbed.

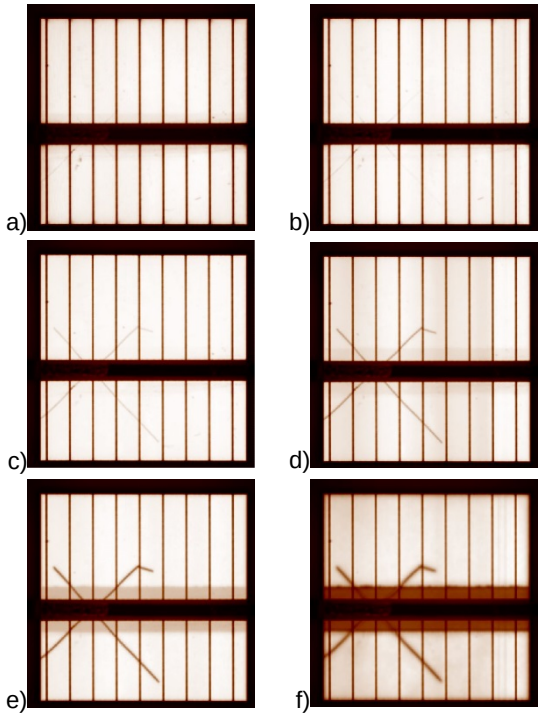

Figure 2: normalized c-Si cell LBIC maps of 6 lasers a) to f) with increasing source wavelength a) 405nm b) 535nm c) 690nm d) 808nm e) 904nm f) 1060nm.

Figure 3 plots the extreme points identified in the active area of local EQE map (excluding fingers and contacts). The average values given are calculated over the total cell area. Thus, the average is partly below the performance of the worst case EQE curve. The crack and the low reflectivity of the back contact cause a sharper drop in the IR region at the worst case point. The average EQE curve compares reasonably well with the EQE curve measured using a dedicated over-illuminating system.

ISBN 0 904963 82 9

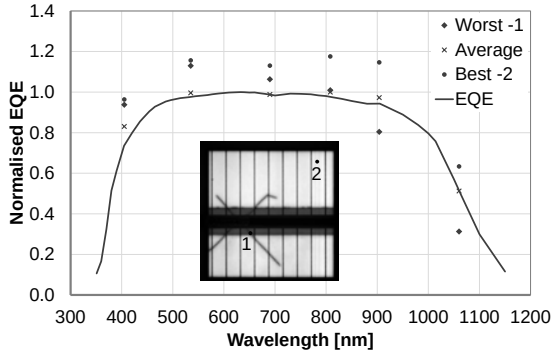

Figure 3: extreme points of local EQE in c-Si sample compared to the local EQE map average and dedicated EQE measurement system results; data is normalized

3.2 a-Si solar cell

The a-Si sample measured is a large area laboratory single cell with an area of 90x60 mm^2. This cell has visible discolouration along the cell length and is darker at the centre and brighter on the outer sides. Thus, it was an ideal cell to investigate non-uniform performance distribution. Measurement resolution was 200µm. The 120k measurements where measured in ~7h.

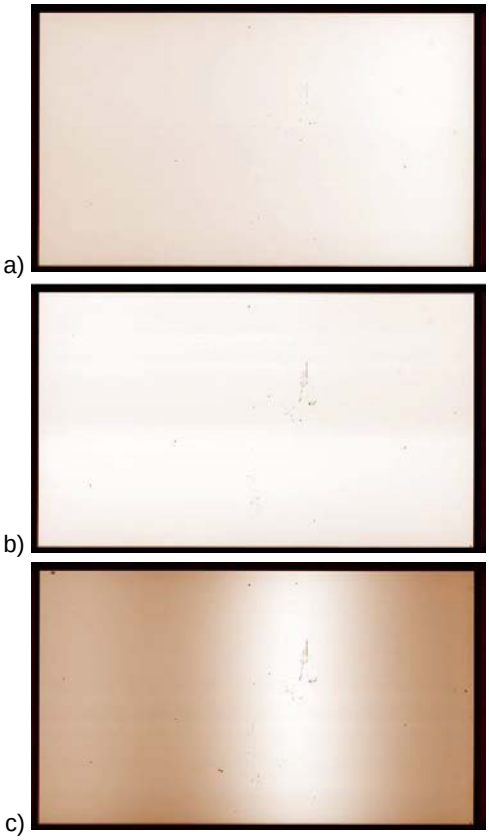

Figure 4: Normalized a-Si sample LBIC maps at a) 405nm b) 535nm and c) 690nm excitation.

Since the a-Si sample only responds up to ~800nm, lasers above that limit did not generate any photocurrent in the cell, thus those have not been plotted in Figure 4. Effects from any discoloration of the cell are not visible in the first two plots, however, large variations are visible in the 690nm laser current map. Those variations match exactly the discoloration of the cell. The white area with the largest current generated corresponds to the darkest area visible on the cell and vice versa.

Although the discoloration of the cell is clearly visible with a naked eye, the 405 and 535nm laser current maps in Figure 4 are not affected by the discoloration. This means that the discoloured areas exhibit pour light trapping so longer wavelengths are not efficiently absorbed. The active layer of the sample is not influenced as demonstrated by the 405 and 535 nm current maps. This is also clear from the EL measurements of this sample (shown in [6]), which do not show the same variations over the width of the cell, making an optical effect more likely.

Another thing to notice in Figure 4 is a defect in the upper right centre of the cell, which is more pronounced at longer wavelength laser light. This defective area is also visible in the EL image, which may indicate a more pronounced failure of the back surface reflector.

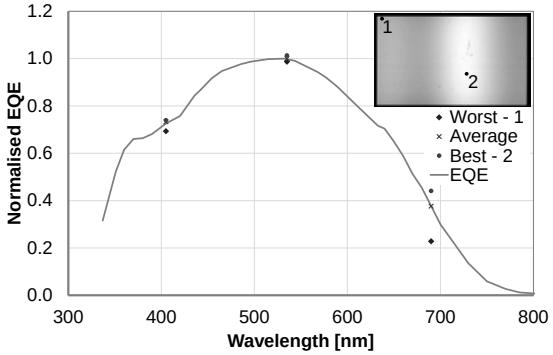

Figure 5: A-Si sample extreme points of local EQE compared to the local EQE map average and dedicated over-illuminating EQE measurement system results; data is normalized to the map average curve.

The average EQE calculated over the active cell area is in good agreement with the normalized EQE measured in a dedicated over--illuminating EQE system as shown in Figure 5.

4 System Development Remarks

Once all diode lasers are operational, the system will have 11 different wavelength laser sources, while the hardware development allows for up to 18 sources. Since diode lasers at other wavelength can be significantly more expensive, LED may be used to complete a ~50nm wavelength resolution SR curve for a sufficiently detailed SR curve.

First tests have shown that the 50-50 beamsplitter used is less than ideal because much of the light intensity needed on the sample

ends up one the reference diode and partly even at the reflectance output. To improve signal strength of the lasers on the sample different options may need to be investigated. At the same time this should also improve the collection efficiency at the reflectance output, which is losing 50% of the signal to the input fibre.

The absolute EQE data scale did not match perfectly between the local EQE map and the EQE from the dedicated system. This is thought to be due to the rather simple preliminary calibration method used and due to the difference in measurement settings (data acquisition time) that have been seen to affect the FFT data extraction. An initial investigation into laser stability has revealed a variability of up to ±2% on the EQE signal, even though the data is stability corrected with the reference. This needs further attention to determine and eliminate the causes.

The laser spot size needs to be investigated at greater detail to determine variation in size at longer wavelength due to chromatic aberrations. First observation show no loss in sharpness of the fingers and busbars of the c-Si cell shown in Figure 2, which means the focusing is good for all wavelengths.

Bias lighting will be needed to properly bias the test cell to a more linear operating area similar to the in-field operating conditions. This would also enable series- and shunt resistance investigations as detailed in [7].

The laser system is integrated into the global electroluminescence (EL) and spectral EL system previously reported in [6]. Thus it is also possible to place a fibre at the third exit leading to the monochromator for spectrally resolved photoluminescence as well as EL measurements, simultaneously acquired with current mapping, further enhancing the characterisation possibilities of the system.

Worth investigating is also the possibility of applying a continues moving YX-stage measurement method as described in [8], which would reduce measurement time considerably.

5 Summary and Future Work

This work has presented an in-house developed multi-laser LBIC system for spatially resolved spectral response measurements of solar cells. Even though, currently only 6 of the 11 Lasers are operational, first test measurements of a c-Si and a-Si solar cell show that the measurement system already delivers valuable device performance details. Measurement results clearly highlight one of the advantages of using localized EQE systems: depth profiling of device performance and defects. In addition, further characterisation options such as diffusion length, minority carrier lifetime and J_{SC} mapping, make it a valuable tool in the field of solar cell materials research and development and in device ageing studies.

The next steps in the development of this system are the assembly of the remaining diode lasers and control hardware. Once fully operational, the measurement characteristics of the system will be investigated and optimised.

Acknowledgements

This work was supported by the UK Engineering and Research Council through the PVteam project EP/L017792/1: Photovoltaic Technology based on Earth Abundant Materials.

References

[1] M. Padilla, B. Michl, B. Thaidigsmann, W. Warta, and M. C. Schubert, “Short-circuit current density mapping for solar cells,” *Sol. Energy Mater. Sol. Cells*, vol. 120, no. PART A, pp. 282–288, Jan. 2014.

[2] P. Vorasayan, T. R. Betts, A. N. Tiwari, and R. Gottschalg, “Multi-laser LBIC system for thin film PV module characterisation,” *Sol. Energy Mater. Sol. Cells*, vol. 93, no. 6–7, pp. 917–921, 2009.

[3] D. L. Young, B. Egaas, S. Pinegar, and P. Stradins, “A new real-time quantum efficiency measurement system,” *2008 33rd IEEE Photovolatic Spec. Conf.*, vol. 80401, pp. 1–3, 2008.

[4] T. Missbach, C. Karcher, and G. Siefer, “Frequency-Division-Multiplex-Based Quantum Efficiency Determination of Solar Cells,” *IEEE J. Photovoltaics*, vol. 6, no. 1, pp. 266–271, Jan. 2016.

[5] J. Carstensen, A. Schütt, G. Popkirov, and H. Föll, “CELLO measurement technique for local identification and characterization of various types of solar cell defects,” *Phys. status solidi*, vol. 8, no. 4, pp. 1342–1346, Apr. 2011.

[6] M. Bliss, X. Wu, K. G. Bedrich, J. W. Bowers, and R. Betts, Thomas Richard Gottschalg, “Spatially and spectrally resolved electroluminescence measurement system for photovoltaic characterisation,” *IET Renew. Power Gener.*, vol. 9, no. 5, pp. 446–452, 2015.

[7] J. Carstensen, G. Popkirov, J. Bahr, and H. Foll, “CELLO: An advanced LBIC measurement technique for solar cell local characterization,” *Sol. Energy Mater. Sol. Cells*, vol. 76, no. 4, pp. 599–611, 2003.

[8] R. M. Geisthardt and J. R. Sites, “Nonuniformity Characterization of CdTe Solar Cells Using LBIC,” *IEEE J. Photovoltaics*, vol. 4, no. 4, pp. 1114–1118, Jul. 2014.